

.....

A Modified Method for Dextrin-capped Gold Nanoparticle Synthesis

Flora M. Yrad

Chemistry Department

Silliman University, Dumaguete City

Dextrin methodology is an aqueous alkaline chemical process for gold nanoparticle (AuNP) synthesis that takes eight long hours of reaction. A modified procedure is hereby described to simplify the procedure and equipment, and reduced the reaction time to only one hour. The key features of the modified protocol are the reversal of the addition of reagents in the original dextrin protocol and the increase of reaction temperature. Optimum synthesis was achieved by sequential neutralization of 50 mL of 2 mM HAuCl_4 with 0.5 mL of 10% Na_2CO_3 and alkaline reduction using selected volumes of 25 g/L dextrin. The AuNPs produced were monodisperse based on dynamic light scattering (DLS) measurements. The surface plasmon resonance band ranged from 517 to 520 nm indicating spherically-shaped AuNPs. High resolution transmission electron microscopy (HRTEM) further confirmed the spherical shape with average sizes from 7.3 ± 1.1 to 18.9 ± 1.5 nm, depending on the volume of dextrin. Chemical reactions are hereby proposed to explain the chemistry of AuNP formation based on the alkaline reduction of $[\text{AuCl}_4]^-$ complex with dextrin as the reducing agent.

Keywords: dextrin, gold nanoparticles, high resolution transmission electron microscopy

INTRODUCTION

Among the noble metal nanoparticles, AuNPs have stimulated tremendous research in the field of biosensors due to their unique optical properties, biocompatibility, and their relatively simple preparation and modification

(Holzinger, Le Goff, & Cosnier, 2014). AuNPs can be prepared by different techniques such as laser ablation (Sylvestre et al., 2004), photo-reduction, γ -radiation, and chemical syntheses (Alzoubi, et al., 2015).

Chemical syntheses are mainly based on the reduction of HAuCl_4 in the presence of a stabilizing agent (Tiwari et al., 2011). Various methods have been developed for the “bottom up” chemical synthesis of AuNP. The Turkevich and the Brust methods are two common techniques for the chemical synthesis of spherical AuNPs. The increasing interest in AuNP research has paved the development of many other chemical methods like synthesis mediation by homopolymer (Zhou et al., 2009), the use of carbon dioxide (Young et al., 2011), carbohydrates (Compostella et al., 2017), and AuCl (Lu et al., 2008). Other published works involved modifications of standard methods to improve techniques, enhance biocompatibility, provide better size control, or for a greener alternative (Zabetakis et al., 2012).

Dextrin methodology was a novel work of the Nano-Biosensors Laboratory, Michigan State University, Michigan, USA. It was developed to provide a greener alternative to the Turkevich method. This method involves synthesis in an alkaline aqueous condition and generates dextrin-capped AuNPs (Anderson et al., 2011). Dextrin-capped AuNPs were reportedly applied in biosensing studies which included AuNP-based biosensors for the detection of *Mycobacterium tuberculosis* (Torres-Chavolla & Alocilja, 2011), dengue-3 virus (Contreras et al., 2016), and unamplified DNA sequence from *Pseudoperonospora cubensis* (Baetsen-Young et al., 2017). Although the dextrin-capped AuNP has shown versatility in some biosensing applications, its synthesis needs improvement because the initial steps involved pH adjustment that are tedious, and the reaction takes eight long hours to complete.

This research aimed to modify the standard dextrin synthesis procedure to improve the method. The modified synthesis conditions such as temperature, amounts of Na_2CO_3 , HAuCl_4 , and dextrin were optimized. UV-Vis spectroscopy, HRTEM, and DLS were used to characterize the morphology, stability, dispersity, and sizes of the dextrin-capped AuNPs.

MATERIALS AND METHODS

Gold (III) chloride trihydrate ($\text{HAuCl}_4 \cdot 3\text{H}_2\text{O}$) and sodium carbonate (Na_2CO_3) were purchased from Sigma-Aldrich. Dextrin ($(\text{C}_6\text{H}_{10}\text{O}_5)_n$) was purchased

from Fluka Analytical. Hydrochloric acid (HCl) and nitric acid (HNO₃) were purchased from EMD Millipore. All chemicals were of analytical grade, and all aqueous solutions were prepared using Type I water (≤ 18.2 M Ω cm) from Direct-Q3 Water Purification System. All glasswares used during synthesis were cleaned with aqua regia (3HCl:HNO₃), rinsed 10 times with Type I water, and dried for 30 minutes in an oven at 120°C. All magnetic bars were soaked in aqua regia and rinsed several times with Type I water.

Modified Synthesis of AuNP

All syntheses were carried out such that the total volume of all reactants (20 mM HAuCl₄, 10 % w/v Na₂CO₃, 25 g/L dextrin) and water, combined together, was 50 mL. A volume of 24.5 mL sterile water was measured and placed into a 125-mL Erlenmeyer flask. Volumes of 5 mL HAuCl₄, 0.5 mL Na₂CO₃, and 20 mL dextrin solutions were added sequentially with swirling of the flask every after addition. The flask was wrapped in aluminum foil and placed on the pre-heated isotherm hotplate/stirrer (Fisher Scientific). All syntheses were performed at constant stirring speed of 525 rpm. At the end of one hour, the mixture was continually stirred for five minutes with the heater off, and then set aside to finally cool down to room temperature. The same procedure was used to separately synthesize AuNPs from different reactant mixtures containing constant 5 mL HAuCl₄ and constant 0.5 mL Na₂CO₃ with varied volumes of water (i.e., 34.5, 39.5, and 42 mL) added with 10, 5, and 2.5 mL of dextrin, respectively. The AuNP product was characterized and stored at 4°C.

Optimization of Synthesis Conditions

Optimum synthesis conditions were investigated by evaluating the effects of Na₂CO₃, hotplate temperature setting, HAuCl₄, and dextrin. In finding the effect of the volume of Na₂CO₃, reaction mixtures containing constant 5 mL HAuCl₄ were neutralized with varied volumes (0.1, 0.25, 0.4, 0.5, 0.6, 0.7, and 1.0 mL) of Na₂CO₃ and reduced with constant 5 mL dextrin, at constant hotplate settings of 150°C. The optimal volume of Na₂CO₃ is that which produced stable colloidal gold. To evaluate the effect of temperature, each of the reaction mixtures containing constant 5 mL HAuCl₄ was neutralized with optimal volume of Na₂CO₃ and reduced with 5 mL dextrin at different hotplate temperature

settings (i.e., 100, 120, 130, 140, and 150°C). To evaluate the effect of dextrin, constant 5 mL of HAuCl_4 was neutralized with optimal volume of Na_2CO_3 and reduced with varying volumes of dextrin (i.e., 2.5, 5, 10, and 20 mL) at constant hotplate settings of 150°C. To evaluate the effect of HAuCl_4 , different volumes of HAuCl_4 (i.e., 1, 2.5, 3, 4, and 5 mL) were neutralized with 0.1, 0.25, 0.3, 0.4, and 0.5 mL Na_2CO_3 , respectively, and were reduced with constant 5 mL dextrin at constant hotplate setting of 150°C.

Characterization of AuNP

The UV–Vis absorption spectra of AuNP were obtained using NanoDrop™ 1000 and One Microvolume UV-Vis Spectrophotometers by Thermo Scientific. The size distribution was evaluated using DLS measurements conducted on a Zetasizer-Nano ZS. A 90° scattering angle, $25 \pm 0.1^\circ\text{C}$ temperature, and a refractive index of 1.4 were considered for all samples during DLS measurements. Particle sizes were obtained from HRTEM and TEM images. HRTEM imaging was performed on JEM-2200FS analytical electron microscope equipped with a 200kV field emission gun (FEG) and in-column energy filter while TEM imaging was performed on JEOL JEM-100CX II operated at 100kV. The AuNP synthesis, UV-Vis spectroscopy, and DLS works were done at the Nano-Biosensors Laboratory, Michigan State University, USA. Both HRTEM and TEM works were done at the Center for Advanced Microscopy, Michigan State University, USA. AuNP mean diameters were calculated using ImageJ software developed at the National Institutes of Health (NIH) (Maryland, USA) available online in the public domain.

RESULTS AND DISCUSSION

The differences between the standard and the modified methods are presented in Table 1. The latter is an inverse synthesis protocol of the former. It is assumed that the inverse protocol involved three stepwise processes, which are neutralization, speciation, and redox reaction. In the first step, the addition of Na_2CO_3 to the mixture containing only water and HAuCl_4 facilitated the neutralization reaction between HAuCl_4 and Na_2CO_3 . In the second step, the Na_2CO_3 exceeding neutralization caused the speciation of gold (III) ions into the forms of $[\text{AuCl}_{4-n}(\text{OH})_n]^-$ complexes where n increases from 0 to 4 as alkalinity

increases. The addition of dextrin in the last step facilitated the alkaline redox reaction between speciated gold (III) ions and dextrin. The addition of dextrin at the last step ensures that the alkaline condition of the reaction mixture can drive the equilibrium towards opening of the hemiacetal rings in the oxidizable ends of dextrin. The facilitation of the stepwise neutralization, speciation, and subsequent reduction explains the increased reproducibility of successful AuNP synthesis in the modified method compared to the standard method.

The reduction of the synthesis time was attributed to the increased temperature of the reaction mixture. As shown in Table 1, the modified method attained a 91°C reaction temperature while the standard method attained only 50°C. It is a general fact that an increase in temperature increases the reaction rate of most of the reactions. This study identified that an increase in reaction temperature was necessary for the HAuCl_4 -dextrin system of AuNP synthesis because while dextrin can undergo oxidation under basic medium, the increase in pH drives the speciation of HAuCl_4 to $[\text{AuCl}_{4-n}(\text{OH})_n]^-$ complexes. It was reported that at pH higher than 6.2, the reactive $[\text{AuCl}_3(\text{OH})]^-$ were converted to less reactive $[\text{AuCl}_2(\text{OH})_2]^-$ and $[\text{AuCl}(\text{OH})_3]^-$ complexes (Ji et al., 2007).

Table 1

Differences between the Standard and the Modified Method

Parameters	Standard method	Modified method
pH adjustment step	Required	Not required
Protocol	Water	Water
	Dextrin	HAuCl_4
	HAuCl_4	Na_2CO_3
	Na_2CO_3	Dextrin
	pH 9 water	
Heating equipment	Hybridization oven shaker incubator Model 136400 Boekel Shake N' Bake	Isotemp hotplate/stirrer (Fisher Scientific)
Temperature setting of heating equipment	50°C	150°C
Highest temperature attained during reaction	50°C	91°C
Stirring speed	100 rpm	525 rpm
Heating time	8 hours	1 hour

Formation of AuNP

The first step in characterizing the formation of AuNP is through visualization of the color of the reaction product. The red color serves as a pointer for a good quality AuNP. In the standard dextrin system, after 8 hours of heating and agitation in the hybridization oven, the reaction product appeared as a red solution (Anderson et al., 2011).

In the modified synthesis system, when 24.5 mL water was combined with 5 mL 20 mM HAuCl_4 , the initial yellow color of HAuCl_4 became lighter because of the dilution effect. Upon the addition of 0.5 mL Na_2CO_3 , the yellow color slowly faded. With the addition of dextrin and swirling, the fading of the yellow color continued. Upon heating, the following series of color change was observed: from very light yellow to grey color that became darker with time, then grey-purple, and finally ruby red. The formation of ruby red color for colloidal gold is consistent with previous reports (Anderson et al., 2011; Zeng et al., 2011). Figure 1 shows the UV-Vis absorption spectra of AuNP by modified method (trial M) compared to the standard method (trial S). Inset of Figure 1 are photo images of reaction products with comparable ruby red color. Both trials M and S were produced from the same reactant compositions of 5 mL HAuCl_4 , 0.5 mL Na_2CO_3 , and 20 mL dextrin.

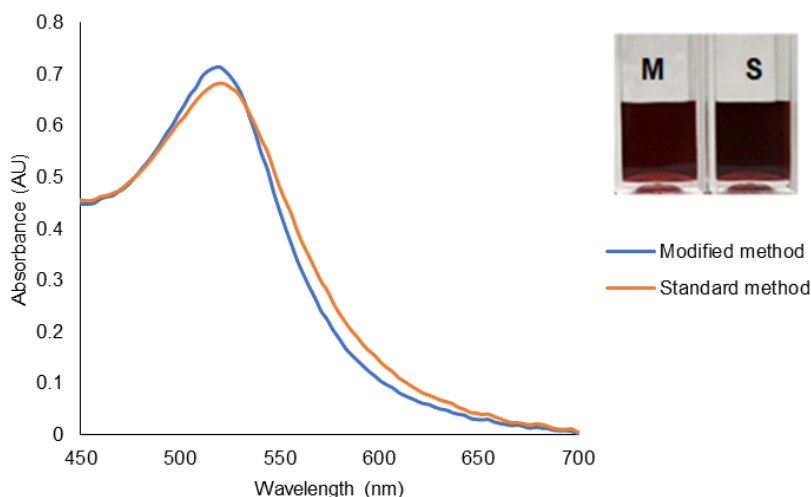


Figure 1. UV-Vis absorption spectra of AuNPs by the modified method (trial M) compared to that of the standard (trial S) (Inset shows vials M and S with comparable ruby red color.)

The spectra of trials M and S as shown in Figure 1 exhibit the same UV-Vis absorption peaks at 520 nm attributed to the surface plasmon resonance (SPR) (Ansari et al., 2015). The similarity in 520 nm maxima (λ_{\max}) of trials M and S explains the similarity in their color, and further suggests that both trials were spherical in shape. Colloidal solutions of spherical AuNPs are red with the SPR band centered at 520 nm (Baptista et al., 2008).

It is noteworthy that the spectral band of trial M was narrow compared to trial S. Narrow SPR band indicates homogeneous gold nanoparticles (Goeken, Subramaniam, & Gill, 2015). By comparison, the spectra of trial M showed a higher peak than that of trial S. According to Beer-Lambert Law which governed molecular spectroscopy, the concentration of the absorbing analyte is linearly related to its absorbance (Skoog et al., 2007). From Figure 1, it can be concluded that synthesis by the modified method yields higher concentration of AuNP compared to that of the standard. Higher absorbance implies higher concentration (Ngo et al., 2016) and therefore higher yield (Jia et al., 2012).

Chemistry of AuNP formation

The chemical reactions involved in the modification are hereby proposed where dextrin served both as reducing and capping agent. These reactions in aqueous solutions are given in equations 1-3.



Dextrin is a low-molecular weight polysaccharide of D-glucose molecules produced by partial hydrolysis of starch (White, Hudson, & Adamson, 2003), and each end of the polymeric chain contains a terminal reducing moiety (Silva et al., 2014). This reducing end is the cyclic hemiacetal ring that can open in aqueous solution to give the reactive aldehyde (CHO) functional group under basic medium. Dextrin with open aldehyde group (RCHO) can be oxidized to carboxylic acid (RCOOH), which in basic medium exists as carboxylate ion (RCOO⁻). The oxidation of dextrin provides the electrons that reduce the

gold (III) ions to Au^0 . The negatively charged carboxylate ion also serves as the capping end of dextrin that stabilized the colloidal gold.

During the synthesis, when Na_2CO_3 was added, hydration produced hydroxyl ions (OH^-) as indicated in Eq. 1. This explains the increase in pH upon addition of Na_2CO_3 . A 50 mL reaction mixture containing 5 mL of HAuCl_4 and 5 mL dextrin had a pH of 2.80 which increased to 3.76 with added 0.1 mL Na_2CO_3 . The pH value showed a further increase as the added volume of Na_2CO_3 increased. Similar reaction mixtures with 0.25 and 0.6 mL of Na_2CO_3 produced pH values of 6.81 and 10.08, respectively.

The OH^- ions served two functions. Firstly, to neutralize HAuCl_4 (Eq. 2) and secondly, to provide alkaline redox medium (Eq. 3). Although gold (III) does not exist as bare ion in aqueous solution but rather as a complex, it is represented as Au^{3+} in Eq. 3. This is to show the stoichiometry of the redox reaction and, more importantly, that it was because of the speciation of gold (III) precursor. Gold (III) precursor from HAuCl_4 can exist in the forms of $[\text{AuCl}_4]^-$, $[\text{AuCl}_3(\text{OH})]^-$, $[\text{AuCl}_2(\text{OH})_2]^-$, $[\text{AuCl}(\text{OH})_3]^-$, or $[\text{Au}(\text{OH})_4]^-$, depending on the pH of the solution (Polte et al., 2010). In aqueous solution, $[\text{AuCl}_4]^-$ undergoes hydration which in turn acts as a weak acid forming $[\text{AuCl}_{4-n}(\text{OH})_n]^-$ where n increases from 0 to 4 as alkalinity increases. In highly alkaline solution, gold (III) can be precipitated as $\text{Au}_2\text{O}_3 \cdot 3\text{H}_2\text{O}$ or $\text{Au}(\text{OH})_3$ (Nicol, Fleming, & Paul, 1987). In their work on Turkevich method mechanism, Ketteman et al. (2016) presented a pH dependent speciation graph of 0.25 mM HAuCl_4 which showed the shift of the gold (III) precursor from $[\text{AuCl}_4]^-$ to $[\text{Au}(\text{OH})_4]^-$ with increasing pH. The said graph illustrates the dominance of $[\text{AuCl}_4]^-$ at pH 2.6 - 5, and the shift to $[\text{AuCl}_{4-n}(\text{OH})_n]^-$ (with $n = 1-3$) at pH 5.6 - 6.8 and finally to a mole fraction of 1 for $[\text{Au}(\text{OH})_4]^-$ at pH 10 (Kettemann et al., 2016). Among the gold (III) species, $[\text{Au}(\text{OH})_4]^-$ is the most stable (Nicol et al., 1987) and has the lowest tendency to be reduced due to its lower reduction potential (Young et al., 2011).

In the present study, stable red AuNPs were produced from reaction mixtures that contained sufficient amount of OH^- ions for both neutralization and alkaline reduction reactions. This was empirically determined to range from $\text{pH} \geq 9.07$ to ≤ 9.88 . This finding is in agreement with the required pH 9 in the standard protocol (Anderson et al., 2011). The importance of this pH 9 requirement can be deduced from the synthesis results of two trials AO and AO-2. Both AO and AO-2 were synthesized from constant 1 mL HAuCl_4 and constant 20 mL dextrin. Trial AO with pH 8.21 gave a pink colored reaction

product while a repeated trial AO-2 with increased volume of Na_2CO_3 gave a pH of 9.64 and produced stable, red colored synthesis product.

Optimization of Reaction Conditions

Effect of Na_2CO_3 . Figure 2 shows the UV-Vis spectra of reaction products synthesized at constant 5 mL HAuCl_4 and constant 5 mL dextrin at varied volumes of Na_2CO_3 (i.e., 0.1, 0.25, 0.3, 0.4, 0.5, 0.6, 0.7, and 1.0 mL). The inset photo of Figure 2 shows products from the different reaction mixtures. Reaction mixture with 0.1 and 0.25 mL Na_2CO_3 produced yellow and bluish solutions, respectively. Although reaction mixture with 0.3 mL Na_2CO_3 produced red solution, the colloidal gold was considered unstable because color separation was observed upon standing. Reaction mixtures with 0.4 and 0.5 mL Na_2CO_3 produced dark red solutions that remained stable even after several months. Synthesis mixtures with 0.6 and 0.7 mL Na_2CO_3 produced black-purple mixture while that with 1.0 mL produced colorless liquid with brown-black precipitate. Based on results, the optimal volumes of Na_2CO_3 were found to be 0.4 and 0.5 mL. Synthesis mixtures with <0.4 or >0.5 mL Na_2CO_3 did not produce stable red colloidal AuNP.

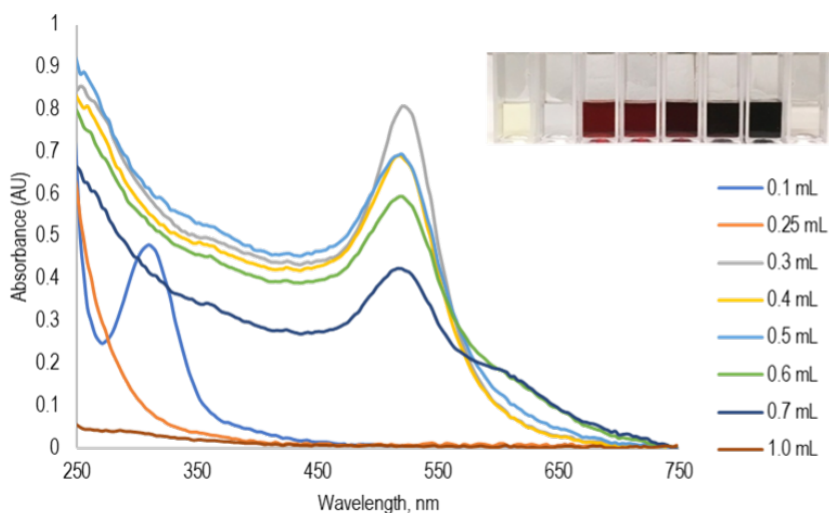


Figure 2. Spectra of AuNP synthesized at constant 5 mL HAuCl_4 and constant 5 mL of dextrin with varied volumes of Na_2CO_3 (0.1, 0.25, 0.3, 0.4, 0.5, 0.6, 0.7, and 1.0 mL) (Inset are photo images of corresponding reaction products at indicated Na_2CO_3 volumes from left to right.)

The effect of Na_2CO_3 volume on AuNP formation can be deduced from their corresponding UV-Vis spectra in figure 2. Reaction mixture containing 0.1 mL Na_2CO_3 with a pH value of 6.81 was a case of insufficient OH^- concentration for neutralization and none for alkaline reduction reaction. Its spectrum shows a peak at λ 313 nm with 0.479 AU attributed to unreacted HAuCl_4 . A 2 mM HAuCl_4 solution gave 0.633 AU at the same wavelength. The HAuCl_4 aqueous solution exhibited UV-Vis absorption peak at 313 nm due to metal-to-ligand charge transfer (King et al., 2015) assigned to $p\sigma \rightarrow 5dx^2-y^2$ ligand-metal transition (Kettemann et al., 2016).

Reaction mixture containing 0.25 mL Na_2CO_3 with a pH value of 6.81 is a case of sufficient OH^- concentration for neutralization but none for alkaline reduction reaction. The absence of needed OH^- for alkaline reduction explains the failure of AuNP formation. Its spectrum lost the 313 nm peak but did not show peak at 520 nm. Instead, it exhibited a steep descending band starting from λ 250 nm with 0.614 AU, sloping down to λ 307 nm with 0.094 AU and runs horizontal thereafter. This band is homologous to previous report involving 0.126 mM HAuCl_4 at pH 6 (Kettemann et al., 2016).

Reaction mixture containing 0.3 mL Na_2CO_3 with pH value of 7.81 is a case of sufficient OH^- concentration for neutralization but insufficient OH^- for alkaline redox reaction. Its spectrum exhibits a 520 nm peak indicating formation of AuNP. While the spectra in Figure 2 shows the highest peak for AuNP synthesized using 0.3 mL Na_2CO_3 , this peak is considered transient because color separation was observed upon standing. The instability of the AuNPs that was initially formed can be attributed to insufficient carboxylate ends of the oxidized dextrin which can cap and stabilize the colloidal gold.

Reaction mixtures containing 0.4 and 0.5 mL Na_2CO_3 with pH 9.14 and 9.77 are cases of sufficient OH^- for both neutralization and alkaline reduction reactions. Both of their spectra exhibited peaks at 520 nm that remained stable even after one year of storage at 4°C. These volumes were considered as optimal.

Reaction mixtures containing 0.6 and 0.7 mL Na_2CO_3 with pH 10.08 and 10.23, respectively, were cases of excessive OH^- ions. At these pH values, the speciation shifted to $[\text{Au}(\text{OH})_4]^-$, and precipitation of $\text{Au}_2\text{O}_3 \cdot 3\text{H}_2\text{O} / \text{Au}(\text{OH})_3$ occurred. The combined stability and lower reduction potential of $[\text{Au}(\text{OH})_4]^-$ slowed down the reduction process. Moreover, the black solids appeared to be the precipitated $\text{Au}_2\text{O}_3 \cdot 3\text{H}_2\text{O} / \text{Au}(\text{OH})_3$ that caused aggregation. The spectra

of both of these trials exhibited broad and low intensity bands at 520 nm. Between pH 10.08 and 10.23, more aggregation is expected from the latter based on speciation and precipitation considerations (Nicol et al., 1987; Nath & Chilkoti, 2004). Experimentally, the latter exhibited absorption band which was broader and much lower 520 nm peak than the former. Reaction mixture containing 1.0 mL Na_2CO_3 with pH 10.69 was a case of very high alkalinity so as to cause complete precipitation of the precursor gold into the form of $\text{Au}_2\text{O}_3 \cdot 3\text{H}_2\text{O}$ or $\text{Au}(\text{OH})_3$ and to give an almost horizontal line spectral band.

Effect of temperature. Using optimized volume of 0.5 mL Na_2CO_3 , reaction mixtures containing the same reactant volumes of 5 mL HAuCl_4 and 5 mL dextrin were heated at different hotplate temperature settings of 100, 120, 130, 140, and 150°C. Among the trials, only reaction products from trial 150°C exhibited the characteristic ruby red color. Reaction product from trial 100°C was purple-red while the rest were light red. From DLS measurements, the polydispersity index (PDI) of trials 100, 120, 130, 140, and 150°C were found to be at 0.139, 0.062, 0.198, 0.208, and 0.068, respectively. Based on PDI classification, AuNPs from trials 100, 130, and 140°C were moderately polydisperse while those from trials 120 and 150°C were narrowly monodisperse (PDI <0.1) (Zabetakis et al., 2012). PDI is a dimensionless number from 0 to 1 calculated from cumulant analysis which is the square of the light scattering polydispersity. This number can be used to describe the non-uniformity of the size distribution of synthesized AuNPs. A low PDI value indicates well dispersed, uniformly sized, and stable gold nanoparticles. A PDI value of 0.087 indicates narrowly monodisperse Au (Hoo et al., 2017). Based on the results, optimal hotplate setting was found to be at 150°C. At this setting, synthesized colloidal gold was ruby red, and it exhibited the highest absorption peak and was highly monodisperse.

Effect of Reaction Time

The progress of reaction was investigated using reaction mixture containing 5mL HAuCl_4 , optimal volume of 0.5 mL Na_2CO_3 , and 5 mL dextrin heated for 1 hour at optimal 150°C hotplate temperature setting. The color, temperature, and UV-Vis spectra of the reaction mixture were monitored with time as the reaction progressed. The reaction mixtures were sampled at 3, 7, 10, 12, 14, 17, 19, 21, 29, 39, 45, and 60 minutes of heating which corresponded to reaction

temperatures of 40, 50, 60, 65, 70, 75, 77, 80, 85, 89, 90, and 91°C, respectively. It was found that from 3-12 minutes of heating, the faint yellow mixture turned grey which darkened with time as the temperature increased from 40-65°C. At 14 minutes of heating, the temperature reached 70°C and the color turned into a very light grey-pink. At 17 minutes of heating, the temperature was 75°C, and the color turned purple. The red color started at 19 minutes of heating at 77°C. From 21 minutes up to one hour of heating, the red color of the mixture remained the same. The highest temperature recorded was 91°C beginning at 57 minutes.

The UV-Vis spectra of the reaction mixture sampled at 14, 17, 19, 21, and 60 minutes demonstrated the evolution of λ_{\max} at 520 nm during the progress of reaction due to plasmon resonance of AuNP. The evolution of λ_{\max} began at 17 minutes (75°C) with a broad band, low intensity peak at 535nm that continuously shifted and increased in intensity as the reaction progressed, until an intense, narrow λ_{\max} at 520 nm was observed at 21 minutes of heating (80°C). This evolution pattern is characteristic of spherical AuNP formation (Zhou et al., 2009). The increase in λ_{\max} intensity is attributed to the increase in volume fraction of Au⁰ as reaction progresses in accordance with Beer's law (Koerner et al., 2012). The absorbances at λ_{\max} 520 nm of the reaction mixture samples were plotted against time and shown in Figure 3.

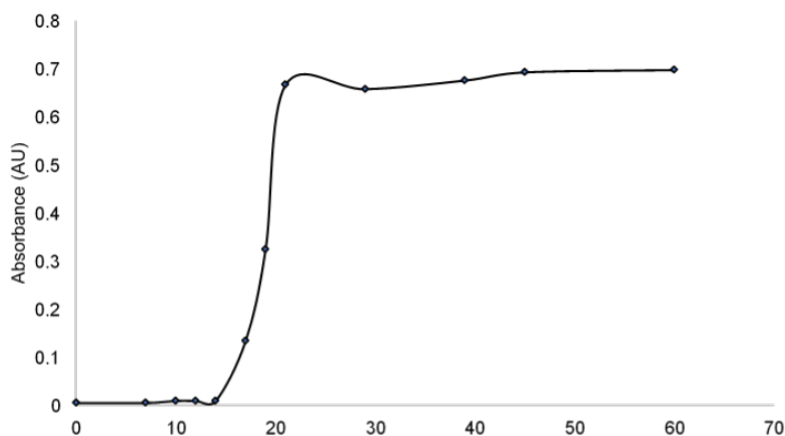


Figure 3. The changes in the UV-Vis absorbance at 520 nm as a function of time

As demonstrated in Figure 3, the absorbances at 520 nm increased with time, reached a maximum at 21 minutes, and made a plateau on the graph thereafter. The curve obtained was comparable to previous reports (Polte et al., 2010; Zhou et al., 2009). The same monitoring of color, temperature, and UV-Vis spectra of the reaction mixture during the progress of reaction was performed for the synthesis of AuNP with 20 mL dextrin. The same curve in Figure 3 was obtained with absorbance at λ_{\max} 520 nm reaching a maximum at 33 minutes that formed a plateau thereafter. Further heating up to one hour did not produce significant changes in the absorbance at λ_{\max} 520 nm. Based on these findings, heating time for the modified method was set at one hour.

Effect of HAuCl_4 . The effect of HAuCl_4 volume was evaluated by preparing AuNPs using constant 5 mL dextrin at varied volumes of HAuCl_4 (5, 4, 3, 2.5, and 1 mL) at an optimal 150°C temperature setting. A volume ratio of 0.1 mL Na_2CO_3 / 1 mL HAuCl_4 was maintained to provide sufficient OH^- ions based on the optimal volume of 0.5 mL Na_2CO_3 in the reaction mixture containing 5 mL HAuCl_4 , as discussed earlier. Figure 4 shows that AuNPs from different volumes of HAuCl_4 exhibited different absorption intensities in their respective spectra at all wavelengths. Clearly, the higher the volume of HAuCl_4 , the higher was the absorption intensity of its spectrum. Notably, despite the differences in their absorption intensities at all wavelengths, all spectra exhibit the same absorption peak at 517 nm. The similarity in λ_{\max} indicates that AuNPs produced from this series of synthesis were not significantly different except for their concentrations based on Beer's Law. AuNPs produced from 5 mL dextrin with 5, 4, 3, 2.5, and 1 mL HAuCl_4 had absorbances of 0.643, 0.51, 0.396, 0.321, and 0.138, respectively.

Inset of Figure 4 shows the reaction products with decreasing intensity of red color as the volume of HAuCl_4 decreased. The decrease in color intensity correlates with their decreasing absorbances at 517 nm. The same series of synthesis was repeated separately for constant volumes of 10 mL and 20 mL of dextrin. The same trend was observed such that the intensity of the AuNP red color also decreased as the volume of HAuCl_4 decreased. It was also observed that regardless of the volume of dextrin, the spectra of AuNP produced from the same $\text{HAuCl}_4/\text{Na}_2\text{CO}_3$ ratio fit was almost identical from 200 nm to 700 nm wavelength range. These results imply that the volume of

HAuCl₄ affects the concentration of generated AuNP. Therefore, HAuCl₄ was the limiting reagent in the reaction.

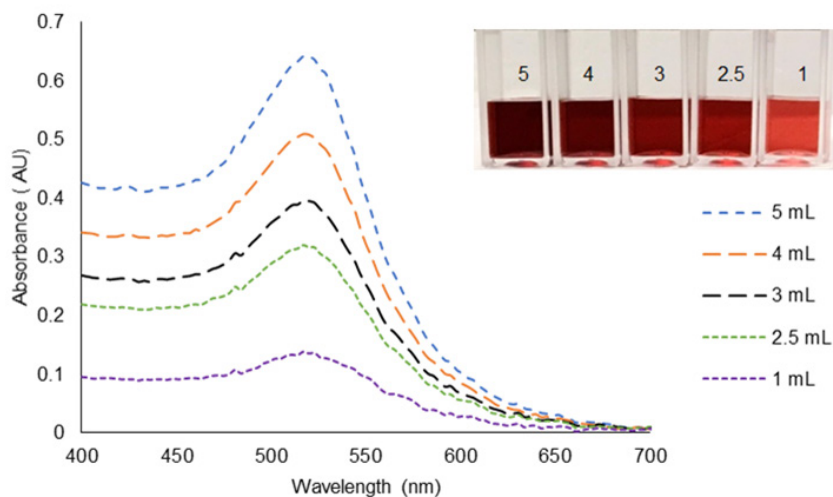


Figure 4. UV-Vis spectra of AuNP at varied volumes of HAuCl₄ (5, 4, 3, 2.5, 1 mL) (Inset shows photo images of AuNPs at the indicated HAuCl₄ volumes.)

Effect of dextrin. The TEM and HRTEM micrographs of AuNPs synthesized from varied volumes (2.5, 5, 10, and 20 mL) of dextrin are shown in Figures 5 A and 5B-D, respectively. They both reveal the spherical shape of AuNPs without aggregation. Reaction products from trials with dextrin volumes of 2.5, 5, 10, and 20 mL produced AuNPs with average sizes of 18.9 ± 1.5 nm, 9.9 ± 1 nm, 8.7 ± 0.5 nm, and 7.3 ± 1.1 nm, respectively. These TEM and HRTEM results correlated with the UV-Vis SPR band as determined to be at 517-520 nm. Spherical AuNP with diameter size <20 nm exhibited SPR from 515-520 nm (Shah et al., 2014). Additionally, Figure 5C shows the lattice fringes and decahedral structure which confirmed the good crystalline nature of the synthesized nanoparticles. These fringes correspond to atomic planes from gold face-centered cubic (fcc) crystal structure (Molina-Trinidad et al., 2011) and are comparable to previous reports (Dkhil et al., 2015; Bankura et al., 2012; Esparza et al., 2008). Another interesting observation in Figure 5C is the clear image of coating around the particle (indicated by the arrow) especially outside the carbon layer support

of the HRTEM grid. This coating appears to be the dextrin that capped the AuNP.

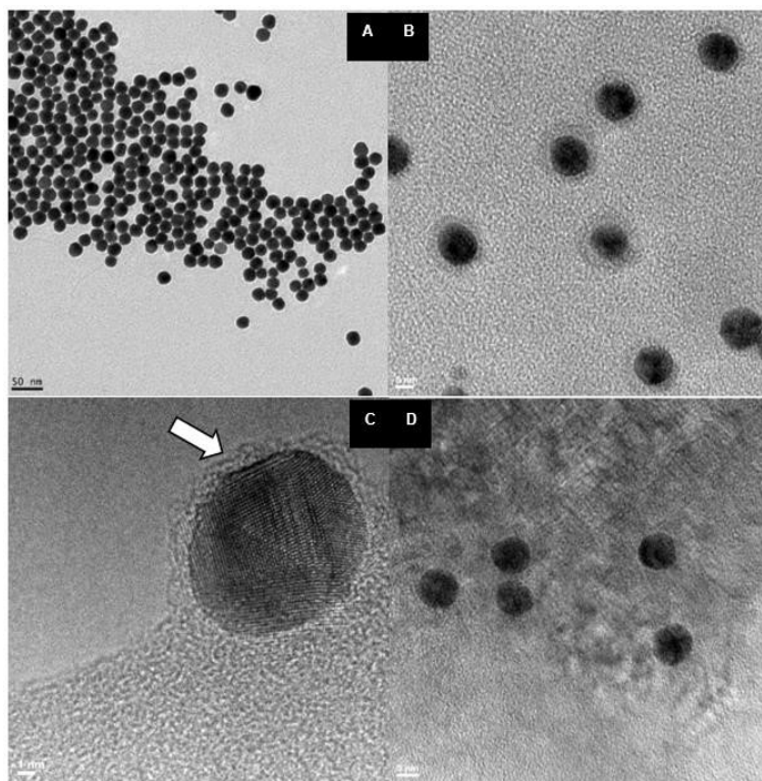


Figure 5. (A) TEM micrograph of 19 nm AuNP from 2.5 mL dextrin (HRTEM micrographs of AuNP: (B)10 nm from 5 mL dextrin, (C) 9 nm from 10 mL dextrin showing fcc crystal fringes and octahedral structure, and (D) 7 nm from 20 mL dextrin)

From HRTEM analysis, the average size of AuNP synthesized by the standard method using 5 mL HAuCl_4 , 0.5 mL Na_2CO_3 , and 5 mL dextrin was found to be 9.8 ± 1.4 nm while that of the modified method was 9.9 ± 1 . T-test results indicated that the mean size difference between the modified and standard method for the same reactant composition was statistically not significant ($p=0.78$). This demonstrates that the dextrin methodology produced AuNPs with controllable size which was dependent on the amount of dextrin.

The sizes of synthesized AuNPs were plotted against the volume ratios of dextrin to HAuCl_4 . Figure 6 shows the varying dependence of AuNP size on the volume ratio of dextrin to HAuCl_4 . It was observed that the mean size of AuNP decreases as the volume of dextrin increases. The observed decrease in AuNP mean size with increasing dextrin concentration is consistent with a previous report (Anderson et al., 2011). A volume ratio of 0.5 produced AuNP size of 18.9 ± 1.5 nm. An increase in the ratio by a factor of 2 decreased the size by a factor of ~ 2 , i.e., from 19.9 ± 1.5 to 9.9 ± 1 nm. However, from the volume ratio of 1, a further increase in the ratio caused little changes in the AuNP size. This finding is consistent with previous observation on modeling study of AuNP citrate method by Kumar, Gandhi, and Kumar (2007). Kumar et al. reported a decrease in size by a factor of 7 when initial concentration ratio of citrate to HAuCl_4 increased by a factor of 5, but a very little decrease in size was observed when the ratio was increased from 2 to 7 (Kumar et al., 2007).

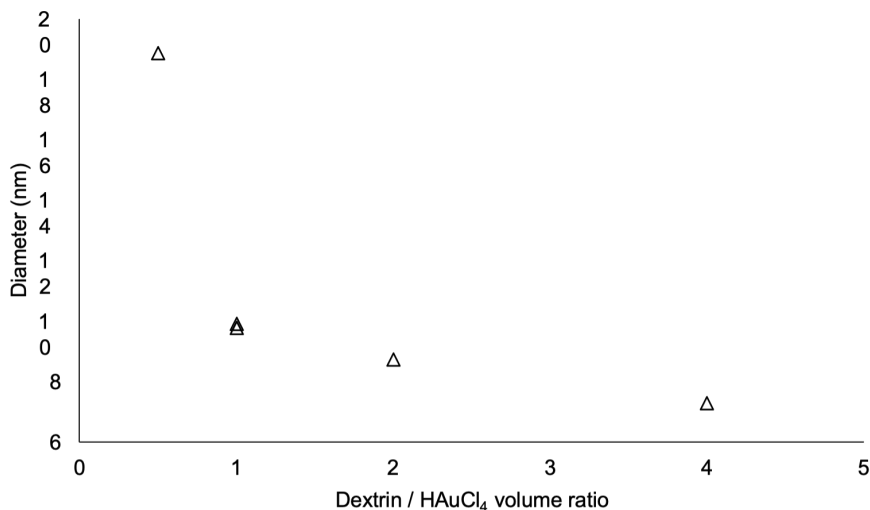


Figure 6. Variation of AuNP size with dextrin / HAuCl_4 volume ratio

Centrifugation of AuNP

While transmission electron microscopy is a well-accepted method for the size analysis of AuNP, centrifugation was explored to see if the latter can

be used to somehow identify the different sizes of dextrin-capped AuNP. Tubes containing 1 mL each of the different sizes of AuNP were centrifuged at varied speed and varied centrifugation time. Figure 7 shows the tubes containing AuNP samples GB, GA, AA, AF, and AK centrifuged for 20 minutes at 12,000 rpm at 4°C. Both trials GB and GA were 19 nm AuNPs while the remaining three trials were 10, 9, and 7 nm core sizes of AuNP, respectively. Centrifugation gathered the AuNP pellets at the bottom of the tubes and the resulting supernatants appeared differently, suggestive of the different sizes. Samples GB and GA with the biggest size (19 nm) produced almost colorless supernatants. The three remaining sizes (10, 9, and 7 nm) produced reddish supernatants that became darker as the AuNP size decreased. These results demonstrate that centrifugation can be used to qualitatively identify the different sizes of dextrin-capped AuNPs based on the appearance of the resulting supernatants.

This simple technique can be very helpful in estimating the sizes of dextrin-capped AuNP in laboratories where TEM instruments are not readily available. Centrifugation is a separation process which involves the use of centrifugal force for the sedimentation of heterogeneous mixtures (Majekodunmi, 2015). It is a separation technique based on the principle of density differences such that particles with higher density than the solvent sink and those with lower density float. In summary, gold nanoparticles were successfully synthesized by modification of the dextrin methodology.

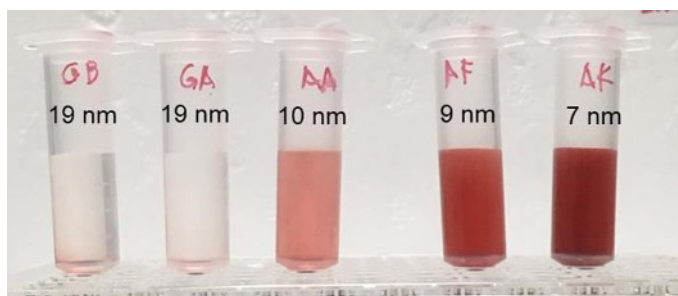


Figure 7. Photo images of the different sizes of dextrin-capped AuNPs after centrifugation for 20 minutes at 12,000 rpm at 4°C (The AuNP pellets gathered at the bottom of the centrifuged tubes and the different colors of supernatants were suggestive of the different sizes of AuNPs.)

CONCLUSION

In conclusion, the standard dextrin protocol for AuNP synthesis was successfully modified. The modification offers a simplified route, substitutes the hybridization oven with less expensive hotplate, and reduces the synthesis time from the eight long hours to only one hour. The size of the AuNPs can be controlled by changing the volume of dextrin. The AuNPs produced were stable, monodispersed and did not show any aggregation even after one year of storage at 4°C. The significant reduction in synthesis time, accompanied by simplified procedure and instrumentation, makes the modified protocol a practical alternative to the standard methodology.

ACKNOWLEDGEMENTS

The author would like to acknowledge Dr. Evangelyn C. Alocilja, Principal Director of the Nano-Biosensors Laboratory, Michigan State University, Michigan, USA for hosting this research, United States Agency for International Development (USAID) for the research funding through its USAID STRIDE Advanced Research Scholarship, and Silliman University for the Faculty Development Committee (FADECO) Doctoral Scholarship.

REFERENCES

- Alzoubi, F., Al-Zouby, J., Alqadi, M., Alshboul, H. A., & Aljarrah, K. (2015). Synthesis and characterization of colloidal gold nanoparticles controlled by the pH and ionic strength. *Chin. J. Phys.*, 53(5), 1–9.
- Anderson, M. J., Torres-Chavolla, E., Castro, B. A., & Alocilja, E. C. (2011). One step alkaline synthesis of biocompatible gold nanoparticles using dextrin as capping agent. *J Nanopart Res* 13(7), 2843–2851.
- Ansari, S. A., Khan, M. M., Ansari, M. O., & Cho, M. H. (2015). Gold nanoparticles sensitized wide and narrow band gap TiO₂ for visible light applications: a comparative study. *New J Chem*, 39(6), 4708–4715.
- Baetsen-Young, A. M., Vasher, M., Matta, L. L., Colgan, P., Alocilja, E. C., & Day, B. (2018). Biosensors and Bioelectronics Direct colorimetric detection of unamplified pathogen DNA by dextrin- capped gold nanoparticles. *Biosens Bioelectron*, 101, 29–36.

- Bankura, K. P., Maity, D., Mollick, M. M. R., Mondal, D., Bhowmick, B., Bain, M. K., & Chattopadhyay, D. (2012). Synthesis, characterization and antimicrobial activity of dextran stabilized silver nanoparticles in aqueous medium. *Carbohydr Polym*, 89(4), 1159–1165.
- Baptista, P., Pereira, E., Eaton, P., Doria, G., Miranda, A., Gomes, I., & Franco, R. (2008). Gold nanoparticles for the development of clinical diagnosis methods. *Anal Bioanal Chem*, 391, 943–950.
- Compostella, F., Pitirollo, O., Silvestri, A., & Polito, L. (2017). Glyco-gold nanoparticles: synthesis and applications. *Beilstein J. Org. Chem*, 13, 1008–1021.
- Contreras, J., Fernando, L., Alocilja, E., Salazar, F., & Bacay, B. (2016). Fabrication of a nanoparticle-based sensor for the detection of dengue virus-3 in aedes aegypti. *IJSBAR* 26(3), 138–157.
- Dkhil, M. A., Bauomy, A. A., Diab, M. S. M., & Al-Quraishy, S. (2015). Antioxidant and hepatoprotective role of gold nanoparticles against murine hepatic schistosomiasis. *Int. J. Nanomedicine* 10, 7467–7475.
- Esparza, R., Rosas, G., Valenzuela, E., Gamboa, S., Pal, U., Pérez, R. (2008). Structural analysis and shape-dependent catalytic activity of Au, Pt and Au / Pt nanoparticles. *Rev Mater*, 13(4), 579–586.
- Goeken, K.L., Subramaniam, V., & Gill, R. (2014). Enhancing spectral shifts of plasmon-coupled noble metal nanoparticles for sensing. *Chem Phys*, 17, 422–427.
- Holzinger, M., Le Goff, A., Cosnier, S. (2014). Nanomaterials for biosensing applications: A review. *Front Chem*, 2(63), 1–10.
- Hoo, X. F., Razak, K. A., Ridhuan, N. S., Nor, N. M., & Zakaria, N. D. (2017). Synthesis of tunable size gold nanoparticles using seeding growth method and its application in glucose sensor. *AIP Conference Proceedings*, 1877, 030001; doi:10.1063/1.4999857
- Jia, H., Gao, X., Chen, Z., Liu, G., Zhang, X., Yan, H., & Zheng, L. (2012). The high yield synthesis and characterization of gold nanoparticles with superior stability and their catalytic activity. *Cryst Eng Comm*, 14(22), 7600–7606.
- Ji, X., Song, X., Li, J., Bai, Y., Yang, W., & Peng, X. (2007). Size control of gold nanocrystals in citrate reduction: The third role of citrate. *J Am Chem Soc*, 129(45), 13939–13948.
- Kettemann, F., Birnbaum, A., Wuithschick, M., Pinna, N., Kraehnert, R., Rademann, K., & Polte, J. (2016). Missing piece of the mechanism of the Turkevich method: The critical role of citrate protonation. *Chem Mater*, 28(11), 4072–4081.
- King, S. R., Massicot, J., & McDonagh, A. M. (2015). A straightforward route to tetrachloroauric acid from gold metal and molecular chlorine for nanoparticle synthesis. *Metals* 5, 1454–1461.
- Koerner, H., Maccuspie, R. I., Park, K., & Vaia, R. A. (2012). In situ UV/Vis, SAXS, and TEM study of single-phase gold nanoparticle growth. *Chem Mater* 24, 981–995.

- Kumar, S., Gandhi, K. S., & Kumar, R. (2007). Modeling of formation of gold nanoparticles by citrate method. *Ind Eng Chem Res*, 46(10), 3128–3136.
- Lu, X., Tuan, H.-Y., Korgel, B. A., & Xia, Y. (2008). Facile synthesis of gold nanoparticles with narrow size distribution by using AuCl or AuBr as the precursor. *Chemistry*, 14(5), 1584–1591.
- Majekodunmi, S.O., (2015). A review on centrifugation in the pharmaceutical industry. *Am J Biomed Eng* 5(2), 67–78.
- Molina-Trinidad, E. M., Estévez-Hernández, O., Rendón, L., Garibay-Febles, V., Reguera, E. (2011). Electronic and vibrational spectra of novel Lanreotide peptide capped gold nanoparticles. *Spectrochim Acta A*, 82(1), 283–289.
- Nath, N., & Chilkoti, A. (2004). Label-free biosensing by surface plasmon resonance of nanoparticles on glass: Optimization of nanoparticle size. *Anal Chem*, 76(18), 5370–5378.
- Nicol, M. J., Fleming, C. A., & Paul, R. L. (1987). The chemistry of the extraction of gold. *The extractive metallurgy of gold in South Africa* (pp. 831-854). Johannesburg: South African Institute of Mining and Metallurgy. Retrieved from <http://www.saimm.co.za/Conferences/ExtractiveMetallurgyOfGold/0831Chapter15.pdf>
- Ngo, V.K.T., Nguyen, D.G., Huynh, T.P., & Lam, Q.V. (2016). A low cost technique for synthesis of gold nanoparticles using microwave heating and its application in signal amplification cation for detecting Escherichia Coli O157: H7 bacteria. *Adv Nat Sci: Nanosci Nanotechnol*, 7, 035016 9.
- Polte, J., Ahner, T.T., Delissen, F., Sokolov, S., Emmerling, F., Thunemann, A.F., & Kraehnert, R. (2010). Mechanism of gold nanoparticle formation in the classical citrate synthesis method derived from coupled in situ XANES and SAXS evaluation. *J Am Chem Soc*, 132 (4), 1296–1301.
- Shah, M., Badwaik, V., Kherde, Y., Waghvani, H.K., Modi, T., Aguilar, Z.P., Rodgers, H., Hamilton, W., Marutharaj, T., Webb, C., Lawrenz, M.B., & Dakshinamurthy, R. (2014). Gold nanoparticles: Various methods of synthesis and antibacterial applications. *Front Biosci*, 19(8), 1320-1344.
- Silva, D. M., Nunes, C., Pereira, I., Moreira, A. S. P., Rosário, M., Domingues, M., & Gama, F. M. (2014). Structural analysis of dextrans and characterization of dextrin-based biomedical hydrogels. *Carbohydr Polym*, 114, 458–466.
- Skooog, D.A., Holler, J.F., & Crouch, S. R. Douglas (2007). *Principle of instrumental analysis*, (6th ed.). Thomson Brooks/Cole.
- Sylvestre, J.P., Kabashin, A.V., Sacher, E. Meunier, M., & Luong, J.H. T. (2004). Stabilization and size control of gold nanoparticles during laser ablation in aqueous cyclodextrins. *J Am Chem Soc*, 126(23), 7176–7177.
- Tiwari, P.M., Vig, K., Dennis, V.A., & Singh, S.R. (2011). Functionalized gold nanoparticles and their biomedical applications. *Nanomaterials*, 1(1), 31–63.

- Torres-Chavolla, E., Alcocilja, E. C. (2011). Nanoparticle based DNA biosensor for tuberculosis detection using thermophilic helicase-dependent isothermal amplification. *Biosens Bioelectron*, 26(11), 4614–4618.
- White, D. R Jr., Hudson, P., Adamson, J. T. (2003). Dextrin characterization by high-performance anion-exchange chromatography -- pulsed amperometric detection and size-exclusion chromatography-- multi-angle light scattering--refractive index detection. *J Chromatogr A*, 997(1–2) 79–85.
- Young, J.K., Lewinski, N.A., Langsner, R.J., Kennedy, L.C., Satyanarayan, A., Nammalvar, V., Lin, A.Y., & Drezek, R.A. (2011). Size-controlled synthesis of monodispersed gold nanoparticles via carbon monoxide gas reduction. *Nanoscale Res Lett*, 6(1) 428.
- Zabetakis, K., Ghann, W. E., Kumar, S., & Daniel, M. C. (2012). Effect of high gold salt concentrations on the size and polydispersity of gold nanoparticles prepared by an extended Turkevich-Frens method. *Gold Bull*, 45, 203–211.
- Zeng, S., Yong, K., & Roy, I. (2011). A review on functionalized gold nanoparticles for biosensing applications. *Plasmonics*, 6, 491–506.
- Zhou, M., Wang, B., Rozynek, Z., Xie, Z., Fossum, J. O., Yu, X., & Raaen, S. (2009). Minute synthesis of extremely stable gold nanoparticles. *Nanotechnology*, 20(50), 505606.